MAJOR AND TRACE ELEMENT VARIATIONS AND LITHOLOGIC COMPONENT ANALYSIS IN APOLLO 17 DRIVE TUBE 73002. M. Neuman[1], P. Koefoed[1], K. Wang[1], B. L. Jolliff[1], R. L. Korotev[1], R. V. Morris[2], and the ANGSA Science Team[3], [1]Department of Earth & Planetary Sciences and the McDonnell Center for the Space Sciences, Washington University in St. Louis, MO 63130, [2]ARES, NASA Johnson Space Center, Houston, TX 77058, [3]www.lpi.usra.edu/ANGSA/teams/ (mdneuman@wustl.edu)

Introduction: A large focus of the Apollo Next Generation Sample Analysis (ANGSA) program is on 73001 and 73002, the double drive tube collected on the "light mantle" at Station 3 during Apollo 17 [1]. The light mantle is thought to represent a landslide deposit off the South Massif, presumably caused by impacting ejecta from Tycho Crater [2]. Exposure ages of rocks from Stations 2 and 3 indicate that the formation of Tycho crater and resulting deposition of the light mantle likely occurred ~100 m. y. ago [3, 4]. Analysis of the Station 3 double drive tube, through ANGSA, provides a unique opportunity to study the light mantle using advancements in technology and knowledge since the early Apollo sample investigations. In this work, we determined the chemistry of every 0.5 cm interval of the 18.5 cm long upper drive tube (73002) and used the chemical compositions to model the proportions of different lithologic components found at the Apollo 17 site.

Methods: We received a total of 37 subsamples of 73002 for this work. Samples were approximately 50 mg of the <1 mm size fraction (dry sieved) from each 0.5 cm increment of dissection Pass 2. Ferromagnetic resonance (FMR) and magnetic measurements were conducted at Johnson Space Center on the samples prior to analyses at Washington University in St. Louis [5]. A small number of large clasts/fragments close to the 1 mm sieving limit visually stood out from the greater portion of fine material. Therefore, we began by grinding and homogenizing each sample in an agate mortar and pestle. Samples were then split into two aliquots: 45 mg for quadrupole inductively coupled plasma-mass spectrometry (ICP-MS), and 5 mg for fused-bead electron-probe microanalysis (FB-EPMA) (see [6] for details).

Results: Elemental concentration variations with depth are prominent for many elements (e.g., Al_2O_3, FeO, TiO_2), while others show more constant values (e.g., SiO_2, MgO, P_2O_5). For many of the elements with affinity for mafic minerals, especially pyroxene and ilmenite (e.g., FeO, TiO_2, Sc, Cr, and V), elevated concentrations are present at the surface of the core in the 0-4 cm intervals (Fig. 1). Several spikes in concentrations of these elements occur in specific intervals that correspond for geochemically similar elements (e.g., 12.5–13.0 cm depth, Fig. 1).

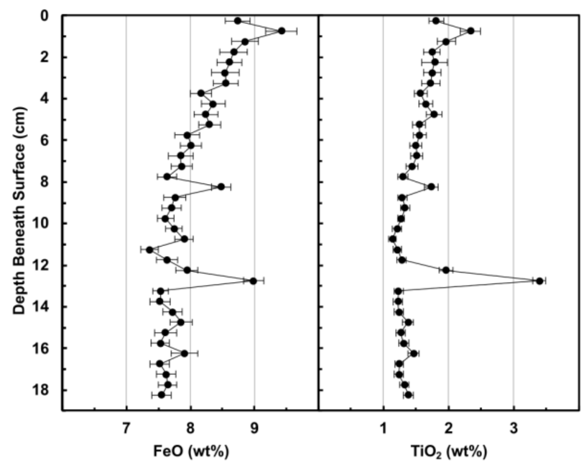

Figure 1. FeO and TiO_2 concentrations of each 73002 core interval from dissection pass 2.

The rare earth elements (REE) have consistent trends of small variations on the scale of the entire core, with slight enrichments of HREEs (heavy-REE) near the surface compared to more uniform LREE (light-REE) values throughout. These variations are expected as the HREE are elevated relative to LREE in the basaltic components. Patterns of the REEs (3 cm averages) are distinct between the upper and lower portions of 73002 (Fig. 2). The near surface composition is simlar to that of 73261, a station-3 trench-sequence soil, and the bottom is similar to 73131, a disaggregated soil clod from Station 2a.

Discussion: Compositions of 73002 intervals show clear trends with depth and many elements with similar geochemical behavior are closely correlated. Given that regolith is a mixture of different lunar materials, we quantitatively determined the proportions of several lithologic components and their variations with depth. We used an error-weighted, linear-least-squares approach that inputs compositions of lithologic components and then determines the proportions of those components by minimizing the sum of squares of residuals, similar to previous studies of Apollo 17 soils [7, 8]. Of all the components provided by [8], we selected high-Ti mare basalt (HT), orange glass (OG), noritic breccia (NB), anorthositic norite (AN), and a volatile-free CI chondrite (CI) to model our samples from 73002. However, we used a CM chondrite composition in place of CI, as CM chondrites have been shown to be the major source of meteoritic material to the lunar surface [e.g., 9].

Results of the mixing analysis show variations in individual elements closely match the variations in the proportions of lithologies (Fig. 3). Anorthositic norite was the most abundant modeled component of 73002 for all intervals, with proportions ranging from 46–63 wt%. Noritic impact-melt breccia and high-Ti mare basalt composed 33–45% and 0.5–13% of the soils, respectively. Orange glass was present in just 16 of 37 intervals, in quantities up to 7 wt%. In cases where the model returned negative results for OG, the model was re-run to exclude this component. Approximately 0.1–2.3% (0.5% average) of the volatile-free CM-chondrite component was needed to resolve the excesses of siderophile elements. Upcoming analysis of 73001 (lower portion of the double drive tube) following the same methods will be paired with the results presented here to provide a comprehensive look at the chemistry of the light mantle deposit.

Acknowledgments: We thank the Preliminary Examination Team (which included MDN and KW) and the curatorial staff at JSC for their work and for allocating the samples, and NASA for supporting ANGSA. In addition, we appreciate assistance from Dr. Paul Carpenter during EPMA sessions.

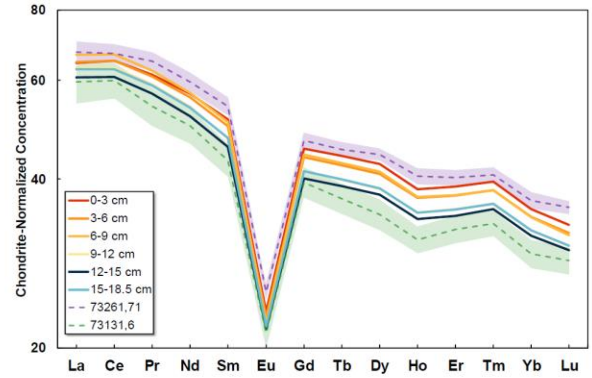

Figure 2. REE patterns for 3 cm averaged sections of 73002. Nearby soils 73261 and 73131 are shown for comparison.

References: [1] Shearer C. K. et al. (2021) *LPSC* **52,** #1566. [2] Howard K. A. (1973) *Science* **180**, 1052–1055. [3] Arvidson R. et al. (1976) *LPSC* **7**, 2817–2832. [4] Drozd R. J. et al. (1977) *LPSC* **8**, 3027–3043. [5] Morris R. V. et al. (2022) *LPSC* **53,** #1849. [6] M. Neuman et al. (2022) *LPSC* **53**, #1567. [7] Boynton W. V. et al. (1975) *LPSC* **6**, 2241–2259. [8] Korotev, R. L., and D. T. Kremser (1992) *LPSC* **22**, 275-301. [9] Wasson J. T. et al. (1975) *The Moon* **13**, 121–141.

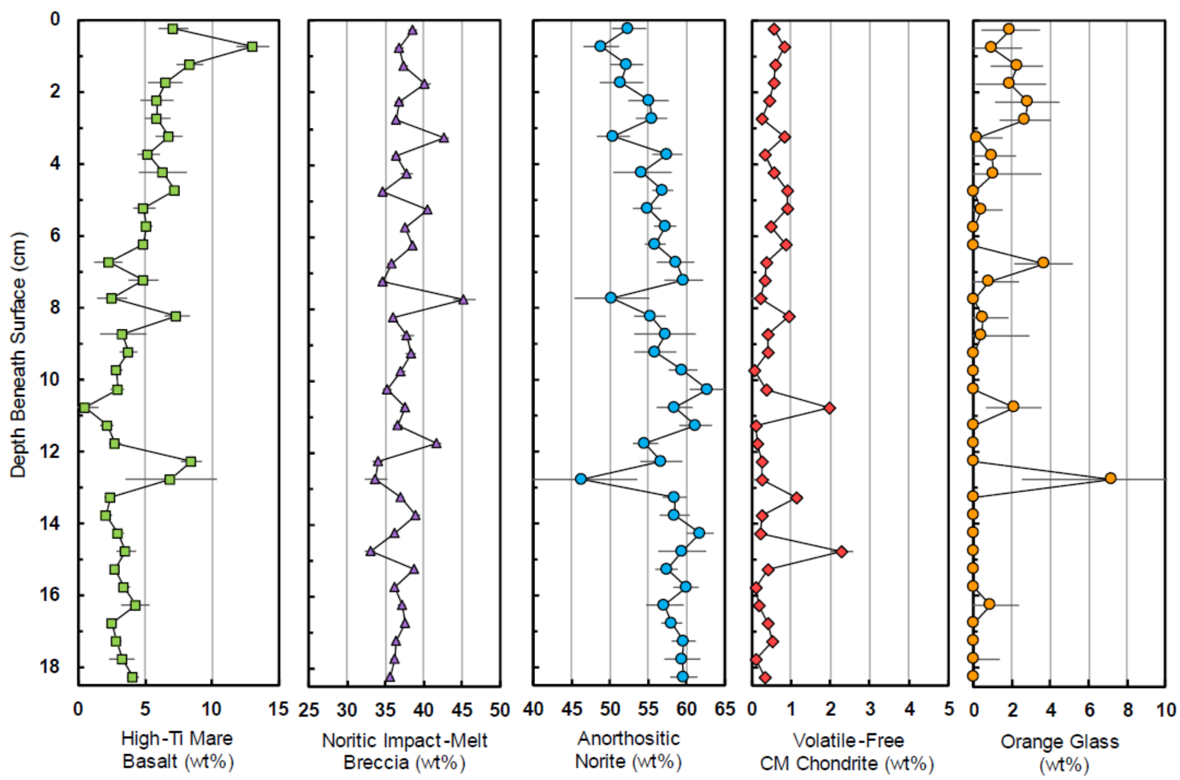

Figure 3. Results of lithologic component mixing calculations.